CASE RECORDS of the MASSACHUSETTS GENERAL HOSPITAL

Case 38-2024: A 22-Year-Old Woman with Headache, Fever, and Respiratory Failure

Eleftherios Mylonakis, M.D., Ph.D., Eric W. Zhang, M.D.,
Philippe B. Bertrand, M.D., Ph.D., M. Edip Gurol, M.D.,
Virginia A. Triant, M.D., M.P.H., and Kristine M. Chaudet, M.D.

From the Department of Medicine, Houston Methodist Hospital, and the Department of Medicine, Weill Cornell Medicine — both in Houston (E.M.); and the Departments of Radiology (E.W.Z.), Medicine (P.B.B., V.A.T.), Neurology (M.E.G.), and Pathology (K.M.C.), Massachusetts General Hospital, and the Departments of Radiology (E.W.Z.), Medicine (P.B.B., V.A.T.), Neurology (M.E.G.), and Pathology (K.M.C.), Harvard Medical School — both in Boston.

N Engl J Med 2024;391:2148-57.
DOI: 10.1056/NEJMcpc2100279

CME

PRESENTATION OF CASE

Dr. Kathleen M. McFadden (Medicine): A 22-year-old woman was transferred to this hospital in the summer before the coronavirus disease 2019 pandemic because of headache, fever, and respiratory failure.

The patient had been in her usual state of health until 8 days before the current presentation, when nausea and myalgias developed. Over the next 2 days, chills, vomiting, neck pain, and headache with sonophobia developed. She presented to the emergency department of another hospital, where an evaluation reportedly showed dry mucous membranes but no signs of meningitis. The white-cell count was 12,300 per microliter (reference range, 4800 to 10,800), and the platelet count was 95,000 per microliter (reference range, 150,000 to 450,000). Intravenous normal saline and morphine were administered, and the patient was discharged with supportive care for a presumed viral syndrome.

During the next week, the patient had worsening headache and new photophobia, as well as malaise, anorexia, nonproductive cough, and dyspnea with minimal exertion. Two days before the current presentation, the patient's mother noticed episodes of confusion with nonsensical speech and excessive sleepiness, and she took the patient back to the emergency department of the other hospital. On evaluation, the patient reported ongoing severe headaches and dyspnea. The temporal temperature was 38.0°C, the heart rate 106 beats per minute, the blood pressure 100/55 mm Hg, the respiratory rate 22 breaths per minute, and the oxygen saturation 97% while she was receiving supplemental oxygen through a nasal cannula at a rate of 2 liters per minute. The patient had photophobia, but the neurologic examination was reportedly otherwise normal. She had mild throat erythema and diffuse abdominal tenderness with intermittent guarding. A urine test for beta human chorionic gonadotropin was negative. Other laboratory test results are shown in Table 1. Blood cultures were obtained.

Computed tomography (CT) of the head, performed without the administration of intravenous contrast material, reportedly showed subarachnoid hemorrhage and

diffuse ischemic changes in the parietal and temporal lobes. Lumbar puncture was deferred because of thrombocytopenia. CT of the chest, abdomen, and pelvis, performed after the administration of intravenous contrast material, reportedly showed diffuse interstitial lung markings, multiple opacities and nodules in the peripheral lung, two hypodensities in the peripheral spleen, and subcentimeter retroperitoneal lymphadenopathy. Empirical treatment with intravenous vancomycin, ceftriaxone, metronidazole, and doxycycline was administered. The patient was admitted to the intensive care unit (ICU) of the other hospital.

The next morning, screening tests for human immunodeficiency virus, Epstein–Barr virus, hepatitis B virus, and hepatitis C virus were negative, as was a blood-smear examination for parasites. Other laboratory test results are shown in Table 1. Platelets were transfused, and intravenous normal saline was administered. The respiratory rate increased to 45 breaths per minute, and the oxygen saturation was 93% while the patient was receiving supplemental oxygen through a nasal cannula at a rate of 8 liters per minute; ventilation with bilevel positive airway pressure was attempted, and intravenous furosemide was administered. Ceftriaxone and metronidazole were discontinued, and empirical treatment with intravenous meropenem and clindamycin was administered. The patient was transferred to the ICU of this hospital.

On arrival at this hospital, the patient had confusion and tachypnea and thus provided a limited history, but family members provided additional information. The patient had a history of depression, for which she received citalopram. She had no known drug allergies. She worked in health care. She drank wine socially, used electronic cigarettes, and occasionally smoked marijuana but did not smoke tobacco. Her most recent travel had been to the Caribbean more than 1 year before the current presentation. She had no exposure to wooded or rural areas. Her family had dogs, but she had no bites or scratches; she had no other animal or insect exposures. There were no recent sexual contacts. Her mother had cutaneous lupus erythematosus, and her maternal grandmother had Hashimoto's thyroiditis.

On examination, the temporal temperature was 37.6°C, the heart rate 97 beats per minute, the blood pressure 103/56 mm Hg, the respiratory rate 49 breaths per minute, and the oxygen saturation 95% while the patient was receiving supplemental oxygen through a nasal cannula at a rate of 8 liters per minute. The body-mass index (the weight in kilograms divided by the square of the height in meters) was 22. The patient appeared to be in respiratory distress, with accessory muscles used for breathing. She was oriented only after prompting. She had meningismus and concomitant rigidity of the shoulders with passive range of motion, but she had no focal cranial-nerve, strength, or sensory deficits. Auscultation of the lungs and heart revealed diffuse rales and rhonchi, as well as a grade 3/6 holosystolic murmur that was loudest at the apex and left axilla and radiated to the sternum. The spleen tip was palpable. A small patch of petechiae was present on the upper chest. The remainder of the examination was normal.

The blood levels of phosphorus, globulin, aspartate aminotransferase, and alanine aminotransferase were normal, as were the results of coagulation tests; antinuclear antibodies were undetectable. Other laboratory test results are shown in Table 1. Additional blood cultures were obtained. Chest radiography showed diffuse lung opacities and pleural effusions on both sides. Electrocardiography showed sinus tachycardia with normal intervals and nonspecific minor ST- and T-wave changes. Empirical treatment with intravenous vancomycin, meropenem, azithromycin, doxycycline, and acyclovir was administered.

Four hours after admission, increased work of breathing, tachypnea, and confusion progressed, and the trachea was intubated for initiation of mechanical ventilation. Intravenous propofol, hydromorphone, and phenylephrine were administered. Bronchoalveolar lavage was performed, revealing mildly bloody and frothy effluent from all the lobes of the lungs. On examination of bronchoalveolar lavage specimens, the nucleated-cell count was 375 per microliter, with 77% neutrophils. Gram's staining showed no organisms. Tests for common respiratory virus — including influenza A and B viruses, respiratory syncytial virus, adenovirus, and parainfluenza viruses — were negative. A culture was also obtained.

Dr. Eric W. Zhang: CT of the head, performed without the administration of intravenous contrast material, revealed bilateral scattered curvilinear hyperdensities in the cortical sulci, findings suggestive of acute subarachnoid hemorrhage (Fig. 1A). There were also focal hypodense regions in the left superior parietal lobule and right temporal lobe with loss of normal gray–white

Table 1. Laboratory Data.*

Variable	Reference Range, Adults, Other Hospital	2 Days before Current Admission, Other Hospital	1 Day before Current Admission, Other Hospital	Reference Range, Adults, This Hospital†	On Current Presentation, This Hospital
Blood					
Hemoglobin (g/dl)	12.0–16.0	12.5	8.8	12.0–16.0	8.9
Hematocrit (%)	37.0–47.0	35.1	25.6	36.0–46.0	25.8
White-cell count (per μl)	4800–10,800	18,910	20,210	4500–11,000	14,640
Differential count (%)					
Neutrophils	37–80	92	89	40–70	91.3
Lymphocytes	10–50	3	4	22–44	5.2
Monocytes	<12	3	4	4–11	3.5
Immature granulocytes	0.0–1.0	1.2	0.7	—	—
Bands	<5	—	3	—	—
Toxic granulation on peripheral-blood smear	Absent	Present	—	Absent	Present
Platelet count (per μl)	150,000–450,000	34,000	28,000	150,000–400,000	90,000
Sodium (mmol/liter)	137–145	133	134	135–145	136
Potassium (mmol/liter)	3.6–5.0	3.4	3.6	3.4–5.0	3.4
Chloride (mmol/liter)	98–107	105	103	100–108	98
Carbon dioxide (mmol/liter)	22–30	30	27	23–32	26
Urea nitrogen (mg/dl)	7–23	25	16	8–25	14
Creatinine (mg/dl)	0.52–1.04	1.03	0.53	0.60–1.50	0.57
Glucose (mg/dl)	65–100	86	94	70–110	103
Calcium (mg/dl)	8.4–10.6	9.0	7.7	8.5–10.5	8.0
Total protein (g/dl)	6.3–8.2	5.7	4.8	6.0–8.3	5.0
Albumin (g/dl)	2.6–5.2	2.6	2.1	3.3–5.0	2.1
Alkaline phosphatase (U/liter)	38–126	169	93	30–100	—
Total bilirubin (mg/dl)	0.2–1.3	1.8	1.1	0.0–1.0	1.0
Direct bilirubin (mg/dl)	—	—	—	0.0–0.4	0.5
Lactate (mmol/liter)	0.70–2.10	2.1	1.4	0.5–2.0	0.9
Lactate dehydrogenase (U/liter)	313–618	785	—	110–210	202
N-terminal pro–B-type natriuretic peptide (pg/ml)	<125	9130	—	—	—
D-Dimer (ng/ml)	—	—	—	<500	1406
Haptoglobin (mg/dl)	—	—	—	30–200	249
Fibrinogen (mg/dl)	—	—	—	150–400	502
Ferritin (μg/liter)	—	—	—	10–200	258
Arterial blood gas					
Fraction of inspired oxygen	—	—	15 liters/min	—	1.0
pH	7.35–7.46	—	7.41	7.35–7.45	7.46
Partial pressure of carbon dioxide (mm Hg)	35–48	—	42	35–42	42
Partial pressure of oxygen (mm Hg)	83–108	—	118	80–100	194
Urine					
Color	Yellow	Yellow	—	Yellow	Amber

Table 1. (Continued.)

Variable	Reference Range, Adults, Other Hospital	2 Days before Current Admission, Other Hospital	1 Day before Current Admission, Other Hospital	Reference Range, Adults, This Hospital†	On Current Presentation, This Hospital
Clarity	Clear	Slightly cloudy	—	Clear	Clear
pH	5.0–9.0	6.0	—	5.0–9.0	6.0
Specific gravity	1.005–1.030	1.010	—	1.001–1.035	1.024
Glucose	Negative	Negative	—	Negative	Negative
Ketones	Negative	Positive (15 mg/dl)	—	Negative	Trace
Leukocyte esterase	Negative	Negative	—	Negative	1+
Nitrite	Negative	Negative	—	Negative	Negative
Protein	Negative	Positive (30 mg/dl)	—	Negative	Negative
Erythrocytes (per high-power field)	0–3	0–3	—	0–2	0–2
Leukocytes (per high-power field)	0–5	16–20	—	<10	<10
Bacteria	Negative	2+	—	Negative	Negative

* To convert the values for urea nitrogen to millimoles per liter, multiply by 0.357. To convert the values for creatinine to micromoles per liter, multiply by 88.4. To convert the values for glucose to millimoles per liter, multiply by 0.05551. To convert the values for calcium to millimoles per liter, multiply by 0.250. To convert the values for bilirubin to micromoles per liter, multiply by 17.1. To convert the values for lactate to milligrams per deciliter, divide by 0.1110.

† Reference values are affected by many variables, including the patient population and the laboratory methods used. The ranges used at Massachusetts General Hospital are for adults who are not pregnant and do not have medical conditions that could affect the results. They may therefore not be appropriate for all patients.

matter differentiation, findings suggestive of acute cortical infarcts (Fig. 1B). CT pulmonary angiography showed evidence of mild interstitial edema, bilateral pleural effusions, and multifocal peribronchovascular nodular opacities and consolidations involving all the lobes of the lungs, some of which were peripherally distributed, without cavitation (Fig. 1C). CT of the abdomen and pelvis showed several splenic hypodensities, which were most likely splenic infarcts, with accompanying mild ascites and mild periportal edema (Fig. 1D).

Dr. McFadden: Platelets were transfused, and lumbar puncture was performed, with an opening pressure of 38 cm of water. On cerebrospinal fluid (CSF) analysis, the glucose level was 41 mg per deciliter (reference range, 50 to 75), the protein level 31 mg per deciliter (reference range, 5 to 55), the red-cell count 2400 per microliter (reference range, 0 to 5), and the nucleated-cell count 49 per microliter (reference range, 0 to 5), with 76% neutrophils, 16% monocytes, and 8% lymphocytes.

Dr. Zhang: Magnetic resonance imaging (MRI) of the head revealed multifocal subarachnoid sulcal hyperintensities on fluid-attenuated inversion recovery (FLAIR) imaging, findings that can be seen with subarachnoid hemorrhage or acute meningitis (Fig. 1E). The focal hypodense regions in the left superior parietal lobule and right temporal lobe that had been noted previously on CT were associated with restricted diffusion on an apparent-diffusion-coefficient map (Fig. 1F) and on diffusion-weighted imaging (Fig. 1G) from MRI of the head, which is compatible with bilateral acute cortical infarcts.

Dr. McFadden: Diagnostic tests were performed, and additional test results were received.

DIFFERENTIAL DIAGNOSIS

Dr. Eleftherios Mylonakis: This previously healthy young woman initially had a constellation of nonspecific symptoms, but then progressive headache with photophobia and neck pain developed, followed by respiratory failure. On evaluation, she had fever, meningismus, a systolic heart murmur, marked thrombocytopenia, and multiple abnormalities on head, chest, and abdominal imaging studies.

THROMBOCYTOPENIA

Thrombocytopenia was an early finding in this patient's disease course and became severe by the time of her second presentation to the other hospital. Pregnancy-related syndromes that are associated with thrombocytopenia — such as HELLP syndrome (characterized by hemolysis, elevated liver-enzyme levels, and a low platelet count) and preeclampsia — are unlikely, given the negative urine test for beta human chorionic gonadotropin. Hemolytic–uremic syndrome and thrombotic thrombocytopenia are important considerations, and the peripheral-blood smear should be examined for evidence of hemolysis. However, the absence of indirect hyperbilirubinemia, a reduced haptoglobin level, and an elevated lactate dehydrogenase level at presentation makes microangiopathic hemolytic anemia (MAHA) resulting from hemolytic–uremic syndrome or thrombotic thrombocytopenia unlikely. MAHA resulting from disseminated intravascular coagulation is also unlikely, especially given the normal results on coagulation testing and the elevated (not reduced) level of fibrinogen.

Thrombocytopenia can be associated with several infections, which are important to consider in this patient, since she presented with fever and leukocytosis. The presence of relative lymphopenia

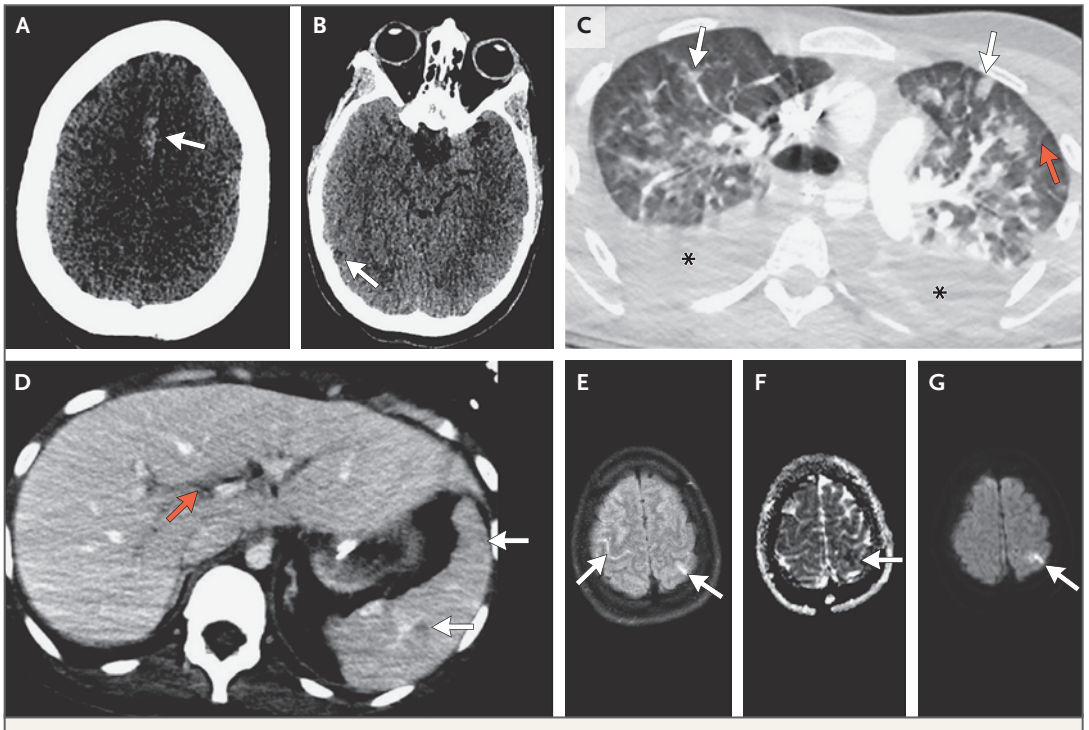

Figure 1. CT and MRI Images.

Non–contrast-enhanced CT of the head shows subtle linear and curvilinear hyperdensities in the cortical sulci at the apex and hemispheric convexities (Panel A, arrow), findings suggestive of acute subarachnoid hemorrhage. Subtle hypodensities in the gray matter along the posterior aspect of the right temporal lobe are suggestive of acute cortical infarcts (Panel B, arrow). CT pulmonary angiography shows multiple peribronchovascular nodular opacities and consolidations involving all the lobes of the lungs (Panel C, white arrows), some of which extend to the subpleural surfaces in the periphery. The presence of associated smooth interlobular thickening bilaterally (Panel C, red arrow) is most likely indicative of mild interstitial edema. Bilateral small-to-moderate pleural effusions are visible (Panel C, asterisks). CT of the abdomen and pelvis shows subtle linear peripheral hypodensities in the spleen (Panel D, white arrows), findings suggestive of splenic infarcts. Mild periportal edema is present in the liver (Panel D, red arrow). MRI of the head shows multiple areas of curvilinear hyperintense signal in the cortical sulci on fluid-attenuated inversion recovery imaging (Panel E, arrows), findings suggestive of subarachnoid hemorrhage or meningitis. The presence of associated focal hypointensity on an apparent-diffusion-coefficient map (Panel F, arrow) and hyperintensity on diffusion-weighted imaging in the left superior parietal lobule (Panel G, arrow) and in the posterior right temporal lobe (not shown) is compatible with acute multiterritorial infarcts.

may suggest a viral infection such as varicella–zoster virus, parvovirus, or cytomegalovirus infection; testing for Epstein–Barr virus, hepatitis C virus, and human immunodeficiency virus was negative. Bacterial infections to consider include leptospirosis and brucellosis, although this patient did not have any known exposures. She presented in the summer, which increases the probability of tickborne infections that are associated with thrombocytopenia, such as Rocky Mountain spotted fever, babesiosis, human monocytic ehrlichiosis, or anaplasmosis. Infective endocarditis can also be associated with thrombocytopenia. Although thrombocytopenia was a prominent finding in this patient, it does not help to narrow the differential diagnosis, so I will consider other key features of her presentation.

HEADACHE, FEVER, AND MENINGISMUS

Headache with photophobia was an early symptom, and confusion, somnolence, and fever later developed. When the patient was transferred to this hospital, she had meningismus, as well as an elevated opening pressure on lumbar puncture and neutrophilic pleocytosis on CSF analysis, despite the administration of antibiotic agents targeting bacterial and viral causes of meningitis. CT of the head, performed without the administration of intravenous contrast material, showed findings suggestive of acute subarachnoid hemorrhage and cortical infarcts. MRI of the head showed high signal intensity within the sulci on FLAIR imaging, a finding consistent with either subarachnoid hemorrhage or meningitis, and also provided confirmation of the multiterritorial infarcts. The patient's clinical presentation could be consistent with meningitis or meningoencephalitis, but why would she also have infarcts?

CORTICAL INFARCTS

Ischemic infarcts are usually caused by arterial occlusion, embolism, or arterial dissection. This patient's imaging showed no evidence of a large intraparenchymal hematoma, a tumor, or arteriovenous transformation. Carotid atherosclerotic disease is unlikely in this young patient; in order for carotid atherosclerotic disease to explain the multiterritorial infarcts, the patient would have to have bilateral disease, which is even less likely. A cardiac source of emboli, such as infective endocarditis, could explain infarcts involving the left parietal lobe and right temporal lobe. In addition, embolic strokes can occur in patients with thrombotic endocarditis due to advanced cancer, systemic lupus erythematosus (Libman–Sacks endocarditis), or antiphospholipid syndrome. Cancer is unlikely in this young patient in the absence of weight loss and imaging findings suggestive of cancer. There was a family history of autoimmune disease, but she had no signs or symptoms suggestive of systemic lupus erythematosus, and testing for antinuclear antibodies was negative.

INFECTIVE ENDOCARDITIS

Could infective endocarditis with septic embolism explain the various aspects of this patient's presentation? A holosystolic murmur may be due to a ventricular septal defect, aortic or pulmonic stenosis, or obstructive cardiomyopathy but is usually caused by atrioventricular valve regurgitation. The murmur observed in this patient was most likely to be caused by mitral regurgitation, given that the typical murmur is heard best at the apex and may radiate to the axilla or precordium. Radiation of the murmur to the sternum may suggest an atypical presentation of mitral regurgitation. In patients with infective endocarditis, mitral regurgitation can result from abnormal leaflet closure caused by either vegetations or perforations of the valve. Mitral-valve vegetations are more likely to become embolic than aortic-valve lesions. Emboli from mitral-valve endocarditis (endocarditis on the left side) could explain both multiterritorial ischemic strokes and splenic infarcts. Congestive heart failure from acute mitral regurgitation could explain the pulmonary edema and elevated level of N-terminal pro–B-type natriuretic peptide that were noted on this patient's presentation, as well as the progression of respiratory failure after the administration of intravenous fluids and blood products. The peripheral pulmonary nodules suggest the possibility of concurrent endocarditis on the right side with septic emboli to the lungs from tricuspid-valve involvement. The nodules involved all the lobes and could also be due to high-grade bacteremia without endocarditis.

Native-valve infective endocarditis should thus be considered in this case. The patient did not have any exposures that would suggest a specific pathogen. She had no history of intravenous drug use, and there was no known recent history of new body piercings that could provide a portal of entry. Overall, streptococci, enterococci, and

staphylococci (*Staphylococcus aureus* and coagulase-negative staphylococci, including *S. lugdunensis*) are the most common pathogens in native-valve infective endocarditis. However, many bacteria, including HACEK organisms (haemophilus species, *Aggregatibacter actinomycetemcomitans*, *Cardiobacterium hominis*, *Eikenella corrodens*, and *Kingella kingae*), are potential pathogens in this case and should be covered with empirical antimicrobial therapy. I would inquire about the results of blood cultures that were obtained before the administration of antibiotics at the other hospital, which would help guide my choice of antimicrobial therapy. I would also perform transthoracic echocardiography to evaluate for vegetations on the mitral valve.

DR. ELEFTHERIOS MYLONAKIS'S DIAGNOSIS

Infective endocarditis with emboli.

DIAGNOSTIC TESTING

Dr. Philippe B. Bertrand: Transthoracic echocardiography was performed and showed normal left and right ventricular size and function. A left pleural effusion was noted. There was superior displacement of the posterior leaflet of the mitral valve that did not meet the criteria for mitral-valve prolapse (Video 1, available with the full text of this article at NEJM.org). On color Doppler imaging, at least moderate, eccentric, anteriorly directed mitral regurgitation was noted (Fig. 2A and Video 2). The left atrial size was normal, which suggested that the mitral regurgitation was not chronic. The eccentricity and anterior direction of the regurgitant jet were compatible with involvement of the posterior leaflet, although no evidence of prolapse or a flail leaflet was seen. Instead, the regurgitant jet appeared to pass through the lateral scallop (P1) of the posterior leaflet, a finding most suggestive of leaflet perforation.

Videos showing echocardiography are available at NEJM.org

A decision was made to proceed with transesophageal echocardiography to characterize the mitral regurgitant jet and evaluate for leaflet perforations and vegetations. Given that the esophagus is located posterior to the left atrium, transesophageal echocardiography is particularly useful in evaluating mitral-valve morphologic features and function. Transesophageal echocardiography revealed two small, mobile echodensities on the atrial surface of the lateral scallop of the posterior leaflet of the mitral valve, findings suggestive of vegetations (Fig. 2B and Video 3). In addition, multiple perforations were noted in the lateral scallop of the posterior leaflet (Fig. 2C and Video 4). The perforations had resulted in an anteriorly directed mitral regurgitant jet that was considered to be severe according to qualitative and quantitative measures (Fig. 2D). There was no evidence of vegetations on the tricuspid or pulmonic valve on either transesophageal or transthoracic echocardiography. On the basis of recommendations from the American College of Cardiology and the American Heart Association, the presence of valve dysfunction resulting in heart failure and the presence of destructive penetrating valve lesions are both indications (class I, level of evidence B) for consideration of early valve surgery, to be performed during the initial hospitalization and before the completion of a full therapeutic course of antibiotics.[1]

Dr. Kristine M. Chaudet: Two sets of blood cultures that had been obtained from the patient before the administration of antibiotics showed growth in the aerobic bottles after 24 hours. Gram's staining revealed the presence of gram-negative coccobacilli. Growth of small colonies was observed on chocolate agar but not on blood agar. An isolate of the organism was sent to the microbiology laboratory at this hospital for analysis by means of MALDI-TOF (matrix-assisted laser desorption ionization–time-of-flight) mass spectrometry, which identified the organism as *Haemophilus parainfluenzae*.

DISCUSSION OF NEUROLOGIC MANAGEMENT

Dr. M. Edip Gurol: About half of patients with infective endocarditis have neurologic symptoms at presentation. Cerebral abscesses and meningitis are not uncommon. Symptomatic neurovascular events can include septic embolism, which could evolve into mycotic aneurysm or brain hemorrhage. Systemic embolism occurs in 22 to 50% of patients with infective endocarditis; the cerebral circulation is affected in two thirds of those cases.[2] The risk of stroke is increased among patients with infective endocarditis who have mitral-valve involvement, especially involvement of the anterior leaflets. *S. aureus*, candida species, and HACEK organisms (including haemophilus species) are

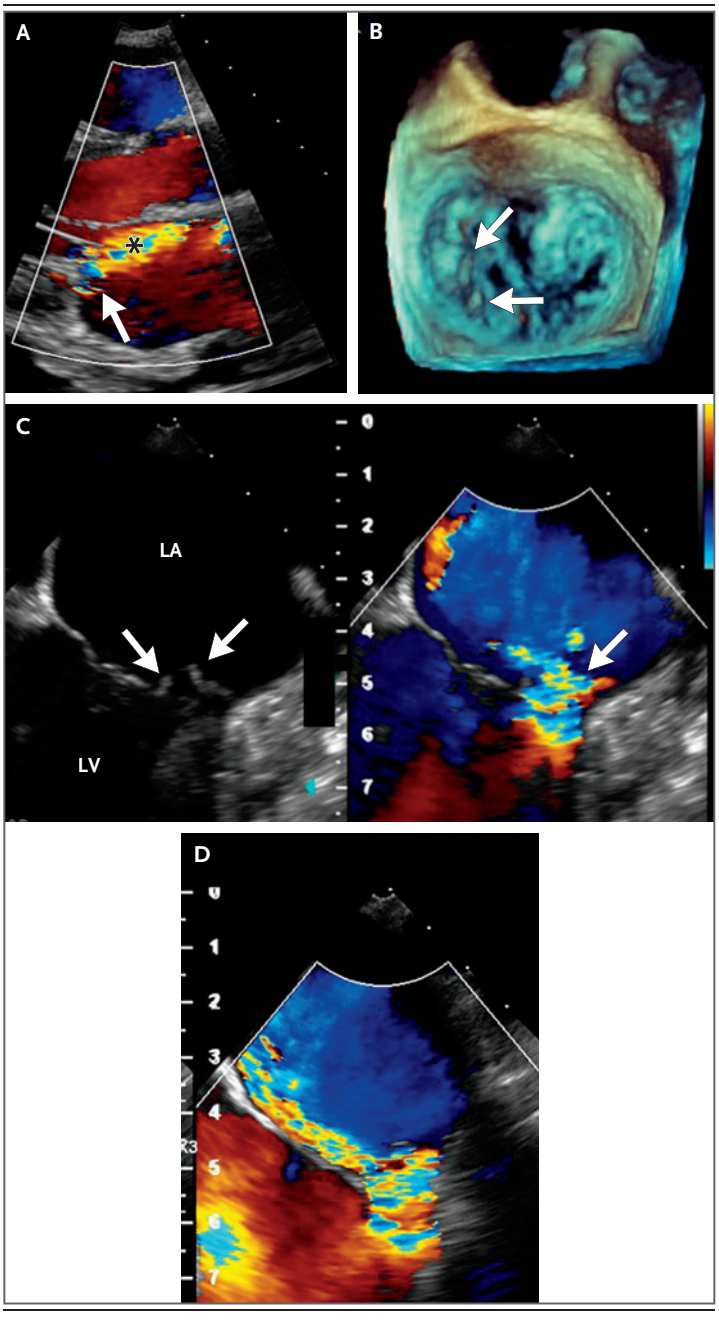

Figure 2. Transthoracic and Transesophageal Echocardiograms.

A transthoracic echocardiogram with color Doppler in the parasternal long-axis view (Panel A) shows eccentric, anteriorly directed mitral regurgitation (asterisk) that appears to pass through the posterior leaflet (arrow). A three-dimensional transesophageal echocardiogram in the "surgeon's view" or "en face view" of the mitral valve (similar to that seen by a surgeon when looking at the mitral valve from the perspective of the left atrium) (Panel B) shows two mobile echodensities (arrows) on the atrial surface of the lateral scallop of the posterior leaflet. A two-dimensional transesophageal echocardiogram in the bicommissural view (omniplane angle, 70 degrees) (Panel C) shows leaflet perforation associated with the mobile echodensities (arrows) on the lateral scallop; LA denotes left atrium and LV left ventricle. A two-dimensional transesophageal echocardiogram with color Doppler in the midesophageal four-chamber view (Panel D) shows mitral regurgitation caused by the perforation, which is considered to be severe according to qualitative and quantitative measures; the jet is directed anteriorly, toward the interatrial septum (left side at the omniplane angle shown in this image).

associated with an increased risk of septic embolism. Anticoagulation has no role in the prevention of septic embolism, and appropriate treatment of the infective endocarditis is key.[2]

This patient had clear evidence of central nervous system (CNS) involvement, including headache, confusion, and signs of meningeal irritation. CT and MRI of the head consistently showed evidence of cerebral infection and inflammation, convexity subarachnoid hemorrhage, microbleeds, and small infarcts. Lumbar puncture confirmed the presence of CNS infection. This clinical and radiologic presentation is the hallmark of septic embolism to the brain with resultant cerebritis as well as ischemic and hemorrhagic lesions.

The presence of subarachnoid hemorrhage was particularly worrisome because it may be related to distal mycotic aneurysm or septic arteritis. Such hemorrhagic complications create a conundrum in the treatment of patients with infective endocarditis and an indication for early valve surgery, which in turn necessitates the administration of high-dose heparin therapy. In patients who have been treated with anticoagulation, the rupture of a cerebral aneurysm can result in catastrophic intracerebral hemorrhage.[3] Thus, in this patient with imaging evidence of subarachnoid hemorrhage, the presence of distal mycotic aneurysm needed to be ruled out. The sensitivity of noninvasive angiographic methods, such as CT angiography and magnetic resonance angiography, for the detection of small (≤3 mm) distal mycotic aneurysms is suboptimal (45 to 85%). For this reason, the patient underwent catheter-based digital subtraction angiography,[4,5] which showed no evidence of mycotic aneurysm. After multidisciplinary discussion among the cardiology, infectious disease, neurology, and cardiac surgery teams, the patient proceeded to valve surgery.

SURGICAL PROCEDURE

Dr. Bertrand: Intraoperative transesophageal echocardiography showed the known leaflet perforation and severe mitral regurgitation. Surgical removal of vegetations and damaged leaflet tissue was performed, followed by reconstruction of the lateral scallop of the posterior leaflet and anterolateral commissure with an autologous pericardial patch. A complete annuloplasty ring was implanted. On imaging performed after the cardiopulmonary bypass, suture material and the autologous patch were noted at the lateral scallop of the posterior leaflet, and the complete annuloplasty ring was well seated (Video 5).

PATHOLOGICAL DISCUSSION

Dr. Chaudet: Microscopic examination of the excised portion of the mitral valve and vegetations revealed fibrin thrombus formation with a neutrophil-rich inflammatory infiltrate (Fig. 3A). Areas of dense inflammation and fibrinoid necrosis were present, with destruction of the normal trilaminar valvular architecture. Clouds of bacterial organisms with indistinct morphologic features were seen on Brown–Hopps staining (Fig. 3B), Grocott methenamine–silver staining, and Steiner staining. Cultures of the mitral-valve specimen showed no growth, most likely because of the antecedent initiation of antibiotic therapy.

DISCUSSION OF INFECTION MANAGEMENT

Dr. Virginia A. Triant: The management of infective endocarditis includes the administration of antimicrobial therapy that is prolonged, parenteral, and bactericidal.[6] Depending on the microorganism, two drugs may be needed to achieve bactericidal activity. Treatment of endocarditis is complicated by the inoculum effect, in which the minimum inhibitory concentration of antimicrobial agents needed to sterilize vegetations is higher than anticipated, particularly for bacterial cell wall–active antibiotics, such as β-lactams and glycopeptides. This effect is thought to be explained by the decreased antimicrobial activity, relatively increased bacterial resistance, and increased likelihood of antibiotic-resistant subpopulations associated with dense bacterial populations.[6] Surgery is often indicated; the decision to perform surgery is influenced by factors such as the microorganism, the size of the vegetations, the presence of perivalvular abscess or valvular regurgitation, and the presence of embolic phenomena.[6-8]

HACEK organisms — a group of gram-negative bacilli that tend to colonize the oropharyngeal tract[6,9,10] — are a relatively uncommon but well-established cause of endocarditis, accounting for an estimated 1 to 10% of cases overall.[8,11] Among HACEK organisms, *H. parainfluenzae* is most likely to cause endocarditis. HACEK endocarditis tends to be a community-acquired illness that affects younger persons as well as those who have recently had an oropharyngeal infection or procedure. HACEK endocarditis is usually a native-valve endocarditis, and it often

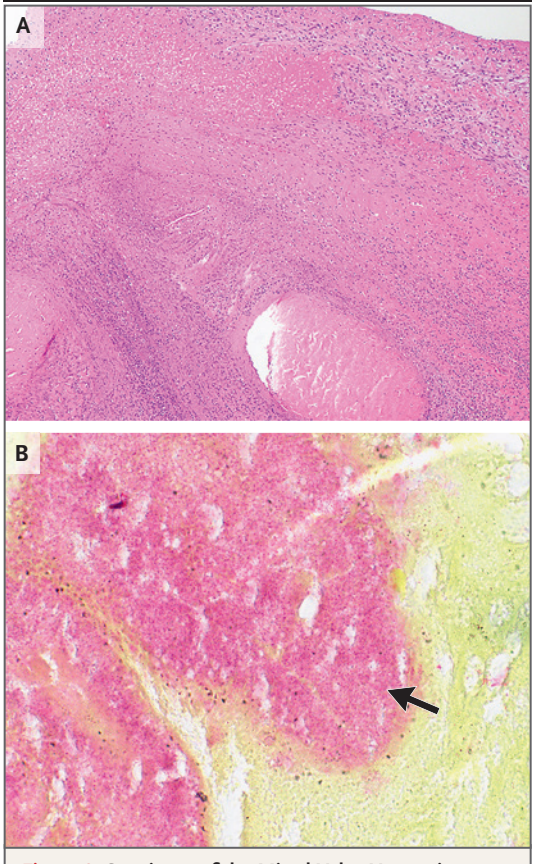

Figure 3. Specimen of the Mitral-Valve Vegetation.
Hematoxylin and eosin staining (Panel A) shows fibrin thrombus with dense neutrophilic inflammation. Brown–Hopps staining (Panel B) shows clouds of gram-negative bacteria with indistinct morphologic features (arrow).

manifests with large vegetations and embolic complications.[10] Stroke is among the common complications and can be embolic or hemorrhagic, resulting from microvascular or immunologic phenomena. Despite the size of the vegetations and the complications observed in patients with HACEK endocarditis, survival tends to be high.[9-11]

Most HACEK organisms are susceptible to third- or fourth-generation cephalosporins, with ceftriaxone being the usual drug of choice.[6,9,10] Strains that produce β-lactamase have decreased susceptibility to ampicillin; in the absence of susceptibility testing, HACEK organisms should be considered resistant to ampicillin and penicillin. Second-line options include ampicillin (if the strain is found to be susceptible) and fluoroquinolones; gentamicin is no longer recommended owing to possible nephrotoxic effects. The duration of treatment is typically 4 weeks for native-valve endocarditis and 6 weeks for prosthetic-valve endocarditis.[6]

When surgery is performed, the first day of treatment is determined by the results of Gram's staining and culture performed on the excised portion of the valve. If Gram's staining or culture is positive (or if perivalvular abscess is present), a full course of antimicrobial therapy is completed after surgery; if Gram's staining and culture are negative, the remainder of the current course of antimicrobial therapy (initiated when the blood culture was found to be positive or the diagnosis of endocarditis was established) is typically completed after surgery.[6] For cases in which a native valve has been replaced with a prosthetic valve or repaired with an annuloplasty ring, there is no consensus regarding whether the duration of treatment should reflect the recommendation for native-valve endocarditis or for prosthetic-valve endocarditis.[6]

In this patient, the *H. parainfluenzae* isolate identified from blood cultures was susceptible to ceftriaxone. She had been treated empirically with broad-spectrum antibiotics, and her treatment was transitioned to ceftriaxone when identification and susceptibility data were available. Because Gram's staining performed on the excised portion of the valve showed bacterial organisms, the patient received ceftriaxone for a total of 6 weeks, including 4 weeks after surgery.

Dr. McFadden: The patient had no cerebral hemorrhagic complications after valvular surgery and had a good neurologic outcome. Seven weeks after surgery, the patient reported having a normal appetite and energy level, and she had returned to her full-time work.

FINAL DIAGNOSIS

Infective endocarditis due to *Haemophilus parainfluenzae*.

This case was presented at the Harvard Medical School course "Internal Medicine Comprehensive Review and Update," directed by Drs. Katrina A. Armstrong, Rocio Hurtado, and David M. Dudzinski.

Disclosure forms provided by the authors are available with the full text of this article at NEJM.org.

REFERENCES

1. Nishimura RA, Otto CM, Bonow RO, et al. 2014 AHA/ACC guideline for the management of patients with valvular heart disease: executive summary: a report of the American College of Cardiology/American Heart Association Task Force on Practice Guidelines. Circulation 2014;129:2440-92.
2. Topcuoglu MA, Liu L, Kim D-E, Gurol ME. Updates on prevention of cardioembolic strokes. J Stroke 2018;20:180-96.
3. Gokcal E, Horn MJ, Gurol ME. The role of biomarkers and neuroimaging in ischemic/hemorrhagic risk assessment for cardiovascular/cerebrovascular disease prevention. Handb Clin Neurol 2021;177:345-57.
4. Graff-Radford J, Fugate JE, Klaas J, Flemming KD, Brown RD, Rabinstein AA. Distinguishing clinical and radiological features of non-traumatic convexal subarachnoid hemorrhage. Eur J Neurol 2016;23:839-46.
5. Yoon NK, McNally S, Taussky P, Park MS. Imaging of cerebral aneurysms: a clinical perspective. Neurovasc Imaging 2016;2:6.
6. Baddour LM, Wilson WR, Bayer AS, et al. Infective endocarditis in adults: diagnosis, antimicrobial therapy, and management of complications: a scientific statement for healthcare professionals from the American Heart Association. Circulation 2015;132:1435-86.
7. Cahill TJ, Baddour LM, Habib G, et al. Challenges in infective endocarditis. J Am Coll Cardiol 2017;69:325-44.
8. Cahill TJ, Prendergast BD. Infective endocarditis. Lancet 2016;387:882-93.
9. Das M, Badley AD, Cockerill FR, Steckelberg JM, Wilson WR. Infective endocarditis caused by HACEK microorganisms. Annu Rev Med 1997;48:25-33.
10. Chambers ST, Murdoch D, Morris A, et al. HACEK infective endocarditis: characteristics and outcomes from a large, multi-national cohort. PLoS One 2013;8(5):e63181.
11. Ambrosioni J, Martinez-Garcia C, Llopis J, et al. HACEK infective endocarditis: epidemiology, clinical features, and outcome: a case-control study. Int J Infect Dis 2018;76:120-5.